

## Electronic and shallow impurity states in a corner

This article has been downloaded from IOPscience. Please scroll down to see the full text article.

1994 J. Phys.: Condens. Matter 6 9729

(<http://iopscience.iop.org/0953-8984/6/45/021>)

View [the table of contents for this issue](#), or go to the [journal homepage](#) for more

### Download details:

IP Address: 171.66.16.151

The article was downloaded on 12/05/2010 at 21:03

Please note that [terms and conditions apply](#).

## Electronic and shallow impurity states in a corner

Zhen-Yan Deng<sup>†‡</sup>, Hong Zhang<sup>†</sup> and Jing-Kun Guo<sup>‡</sup>

<sup>†</sup> Chinese Center of Advanced Science and Technology (World Laboratory), PO Box 8730, Beijing 100080, People's Republic of China

<sup>‡</sup> The State Key Laboratory of High Performance Ceramics and Superfine Microstructure, Shanghai Institute of Ceramics, Chinese Academy of Science, Shanghai 200050, People's Republic of China

Received 24 May 1994, in final form 18 August 1994

**Abstract.** The electronic and impurity states in the corner of well material surrounded by barrier material are investigated using the variational method. The results show that the binding energies of impurity ground states tend to the value of the third impurity excited states in the bulk when the impurity approaches the corner. The dependence of the ground-state electronic level and impurity binding energy on the dielectric mismatch between the well material and barrier material is also discussed.

### 1. Introduction

With the development of microfabrication, it is possible to confine the carriers moving in two directions and in one direction (quantum wells and quantum wires, respectively). Studies of shallow impurity states in these low-dimensional systems have attracted considerable attention. The interfaces in these structures play an important role in determining their electronic and optical properties. Usually, step structures exist at the interfaces [1–7], which affect the optical transition spectra considerably. Tanaka and Sahaki [4] and Tsuchiya *et al* [5] studied  $\text{Ga}_{1-x}\text{Al}_x\text{As}/\text{GaAs}$  quantum wells with periodic stepped interfaces and observed a strong optical anisotropy associated with the interface step structures. Namba *et al* [7] studied the Ni (7 9 11) surfaces by angle-resolved photoelectron spectroscopy and found that a surface local state existed at step edges on Ni (7 9 11) surfaces. In fact, a stepped surface or V-shaped grooves in the interfaces can be viewed as a corner; this model has been used by Lee and Antoniewicz [8, 9] in studying the surface bound states and surface polaron states.

In this paper, we investigate the electronic and shallow impurity states in the corner of two orthogonal surfaces, where the well material is inside the corner and the barrier material is outside the corner. In our considerations, the dielectric mismatch between the well material and barrier material is included, and the electron-confining potential outside the corner is assumed to be infinite. Also, the effective-mass approximation and the variational method are adopted.

The paper is organized as follows. In section 2, we study the electronic states. In section 3, we study the shallow impurity states. The numerical results and discussion are presented in section 4.

## 2. Electronic states

Let us consider a corner of well material of dielectric constant  $\epsilon_1$  surrounded by the barrier material of dielectric constant  $\epsilon_2$ , as shown in figure 1. In the effective-mass approximation, the Hamiltonian for electronic states considering the dielectric mismatch in the corner can be written

$$H^{(0)}(\mathbf{r}) = \frac{|\mathbf{P}|^2}{2m} + V_e(\mathbf{r}) + V(\mathbf{r}) \quad (1)$$

where  $\mathbf{P}$  and  $\mathbf{r}$  are the electron momentum and coordinate, respectively, and  $m$  is the electron-band effective mass. The electron-confining potential well and the electron image potential in the corner are given by

$$V(\mathbf{r}) = \begin{cases} 0 & x > 0, y > 0 \\ \infty & \text{elsewhere} \end{cases} \quad (2)$$

and

$$V_e(\mathbf{r}) = \frac{pe^2}{4\epsilon_1 x} + \frac{pe^2}{4\epsilon_1 y} + \frac{p^2 e^2}{4\epsilon_1 (x^2 + y^2)^{1/2}} \quad \text{for } x > 0, y > 0 \quad (3)$$

where

$$p = \frac{\epsilon_1 - \epsilon_2}{\epsilon_1 + \epsilon_2} = \frac{\epsilon - 1}{\epsilon + 1} \quad (4)$$

is a representation of the dielectric mismatch between the well material and barrier material, with  $\epsilon = \epsilon_1/\epsilon_2$  the ratio of the dielectric constant inside the corner to that outside the corner.

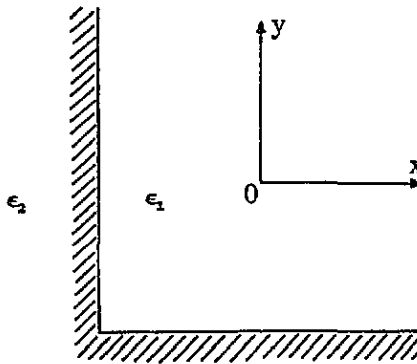


Figure 1. The schematic representation of a corner, where the well material and barrier material are inside and outside the corner, respectively.

2.1.  $p \geq 0$

In the case of when  $p \geq 0$ , i.e.  $\epsilon_1/\epsilon_2 \geq 1$ , the electron image potential is positive (this can be seen from equation (3)), and no localized electronic states exist in the corner. As the simplest approximation, the electronic wavefunction for the Hamiltonian  $H^{(0)}(r)$  can be written

$$\phi(r) = N_0 \sin(k_x x) \sin(k_y y) \exp(ik_z z) \tag{5}$$

where  $N_0$  is the normalization constant and the electron energy is given by

$$E = \frac{\hbar^2}{2m} (k_x^2 + k_y^2 + k_z^2). \tag{6}$$

The ground-state wavefunction and energy level are

$$\phi_0(r) = 0 \tag{7a}$$

$$E_0 = 0. \tag{7b}$$

2.2.  $p < 0$

In the case when  $p < 0$ , i.e.  $\epsilon_1/\epsilon_2 < 1$ , the electron image potential in the corner is negative, and localized electronic states exist in the corner. As in [8, 9], the following trial wavefunction for the electronic ground state is adopted:

$$\phi_0(r) = N_0 xy \exp[-(x + y)/\alpha] \tag{8}$$

where  $\alpha$  is the variational parameter. The electronic ground-state level is obtained as follows:

$$E_0 = \min_{\alpha} (\phi_0(r) | H^{(0)}(r) | \phi_0(r)). \tag{9}$$

3. Impurity states

When the impurity is placed at the position  $(x_0, y_0, 0)$  inside the corner, the Hamiltonian for impurity states can be written

$$H(r) = \frac{|P|^2}{2m} + V_{\text{ion}}(r) + V_e(r) + V(r) \tag{10}$$

where

$$V_{\text{ion}}(r) = -\frac{e^2}{\epsilon_1 [(x - x_0)^2 + (y - y_0)^2 + z^2]^{1/2}} - \frac{pe^2}{\epsilon_1 [(x + x_0)^2 + (y - y_0)^2 + z^2]^{1/2}} - \frac{pe^2}{\epsilon_1 [(x - x_0)^2 + (y + y_0)^2 + z^2]^{1/2}} - \frac{p^2 e^2}{\epsilon_1 [(x + x_0)^2 + (y + y_0)^2 + z^2]^{1/2}}$$

for  $x > 0, y > 0$

(11)

is the sum of the impurity ion potential and its image potentials inside the corner.

From equations (5) and (8), we can see that the first term of the expansion series of electronic wavefunctions is proportional to  $xy$  when  $x$  and  $y$  are small, and the image potentials are small compared with the impurity ion potential; so the trial wavefunction for the impurity ground state that we use is written

$$\psi(\mathbf{r}) = N \frac{xy}{x^2 + y^2 + \beta^2} \exp\left(\frac{-[(x - x_0)^2 + (y - y_0)^2 + z^2]^{1/2}}{\lambda}\right) \quad (12)$$

where  $N$  is the normalization constant, and  $\beta$  and  $\lambda$  are the variational parameters. Equation (12) satisfies the boundary conditions.

As usual, the impurity binding energy is defined as the energy difference between the bottom of the electronic conduction band without the impurity and the ground-state level of impurity states in the corner:

$$E_1 = E_0 - \min_{\beta, \lambda} \langle \psi(\mathbf{r}) | H(\mathbf{r}) | \psi(\mathbf{r}) \rangle. \quad (13)$$

The above integral was calculated numerically.

#### 4. Results and discussion

Figure 2 shows the dependence of the ground-state energy level for localized electronic states on the dielectric mismatch  $p$  between the well material and barrier material. For simplicity, the energy is in units of effective rydbergs,  $\text{Ryd}^* = me^4/2\hbar^2\epsilon_1^2$ , and length is normalized to the effective Bohr radius  $a_0^* = \hbar^2\epsilon_1/me^2$ . In figure 2, we can see that the ground-state energy level increases with increase in the dielectric mismatch  $p$  (absolute value).

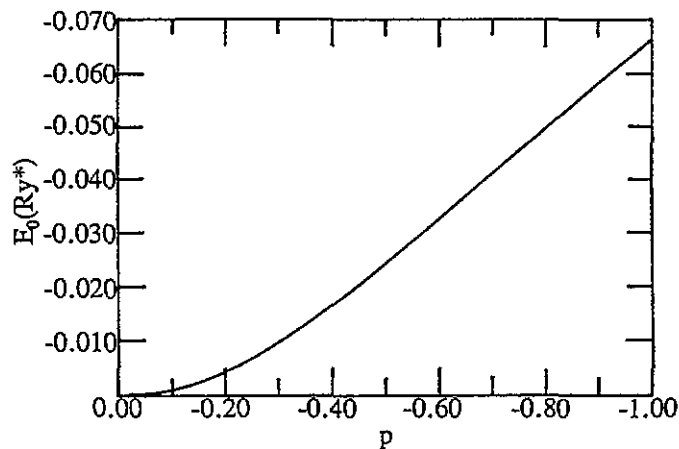


Figure 2. Variations in the ground-state electronic level with the dielectric mismatch  $p$  between the well material and barrier material.

Figure 3 shows the dependence of the impurity binding energy on the impurity position along the central line and one side of the corner for different dielectric constant ratios  $\epsilon$ . In figure 3(a), it can be easily seen that, when the impurity position  $x_0 = y_0$  is reduced, the impurity binding energy decreases and, when the impurity position is near the corner, the impurity binding energy for dielectric constant ratio  $\epsilon = 1$  tends to the value  $\frac{1}{9}\text{Ryd}^*$  of the third impurity excited states in the bulk. From figure 3(a), we can also see that the impurity binding energy increases with increase in the dielectric constant ratio  $\epsilon$  and, when the impurity position is far from the corner, the impurity binding energy approaches the binding energy in the bulk. Figure 3(b) also indicates that, when the impurity position is far from the corner and near one side of it, the impurity binding energy tends to the corresponding binding energy of the impurity near the interfaces of two semi-infinite materials [10].

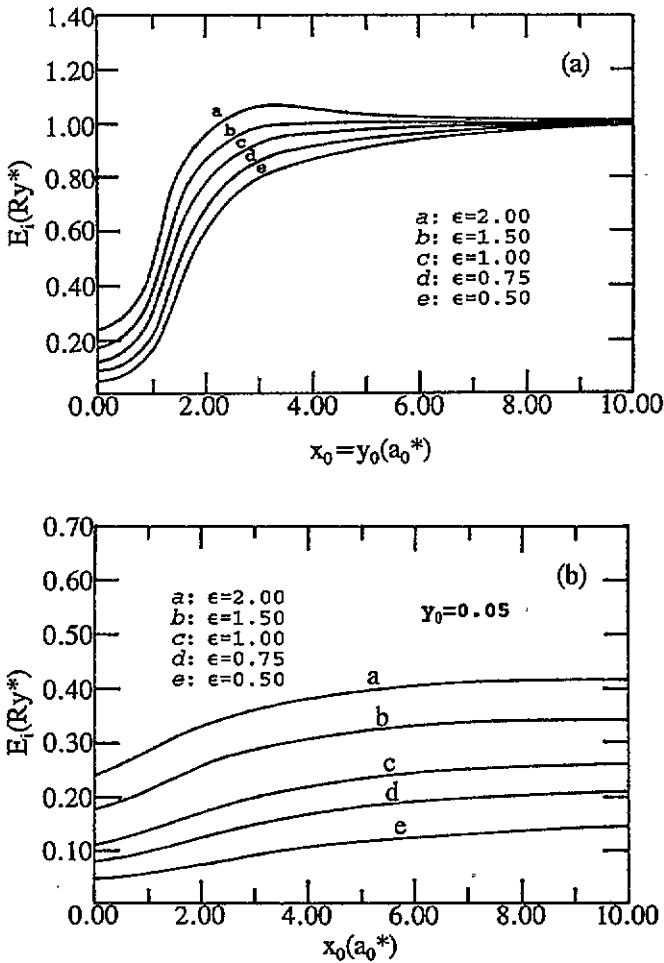


Figure 3. Variations in the impurity binding energy with the impurity position along (a) the central line and (b) one side of the corner for different dielectric constant ratios  $\epsilon$ .

Figure 4 shows the dependence of the impurity binding energy on the impurity position along the central line and one side of the corner for two different semiconductor structures.

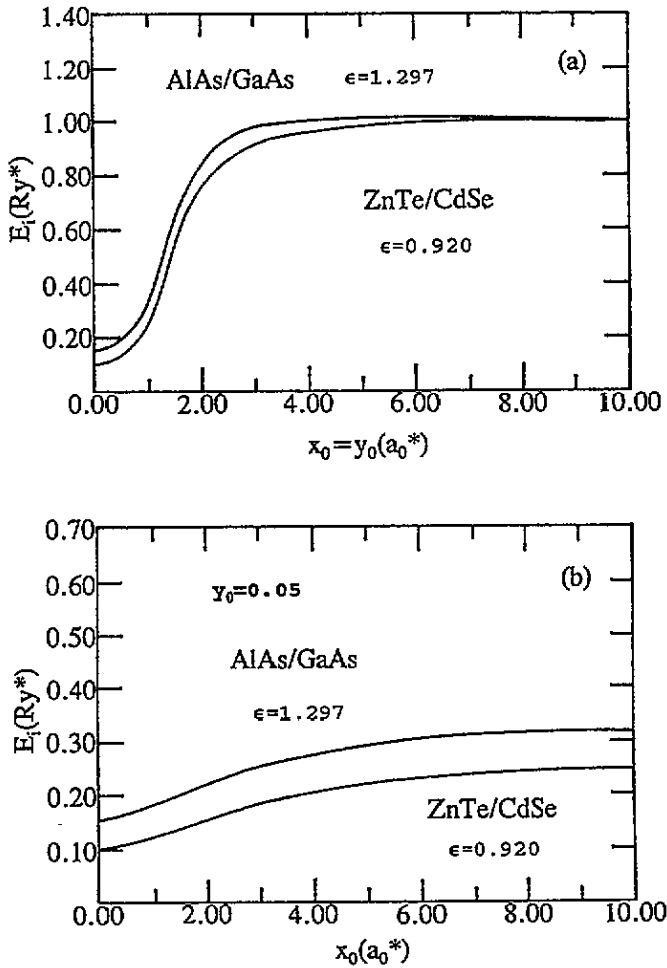


Figure 4. Variations in the impurity binding energy with the impurity position along (a) the central line and (b) one side of the AlAs/GaAs and ZnTe/CdSe corners.

In our calculation, the following parameters are used:  $\epsilon_1 = 13.1\epsilon_0$  and  $\epsilon_2 = 10.1\epsilon_0$  are the static dielectric constants for a GaAs/AlAs corner [11],  $\epsilon_1 = 9.29\epsilon_0$  and  $\epsilon_2 = 10.1\epsilon_0$  are the static dielectric constants for a CdSe/ZnTe corner [12];  $Ryd^* = 5.83$  meV and  $a_0^* = 98.7$  Å for shallow donors in GaAs [11], and  $Ryd^* = 25.95$  meV and  $a_0 = 31.26$  Å for shallow donors in CdSe [12]. Because of the electron-confining potentials  $V_0 \approx 200 Ryd^*$  for the conduction band in AlAs/GaAs [13, 14] and  $V_0 \approx 40 Ryd^*$  for the conduction band in ZnTe/CdSe [15], which are much larger than the impurity binding energies in the corners, the infinite-barrier approximation in the calculation is reasonable. The variations in impurity binding energy with impurity position in figure 4 are similar to those in figure 3, and the corresponding binding energies (in units of effective rydbergs) for AlAs/GaAs are larger than those for ZnTe/CdSe.

The results obtained above are interesting and their physical interpretation and discussion are as follows. When the dielectric mismatch  $p$  between the well material and the barrier material is negative, the image potentials imposed on the electron are attractive, as shown

in equation (3), and localized electronic states exist in the corners [8,9]. On the other hand, the electron image potentials increase with increase in the dielectric mismatch  $p$ , and the ground-state energy level for localized electronic states increases when the dielectric mismatch becomes large (absolute value). Because of the confinement of the electron in the corner, the electronic wavefunctions near the corner for impurity states are very different from those in the bulk and, when the impurity approaches the corner, its wavefunctions are very similar to that of the  $3d_{xy}$  impurity excited state in the bulk which has been shown in equation (12); so the impurity binding energy in the corner tends to the value  $\frac{1}{9}\text{Ryd}^*$  of the third impurity excited states in the bulk. From equation (11), we can see that the impurity ion image potentials vary with the dielectric mismatch  $p$ . When the dielectric constant ratio changes from  $\epsilon < 1$  to  $\epsilon > 1$ , the dielectric mismatch varies from  $p < 0$  to  $p > 0$  and the impurity ion image potentials change from positive to negative. This is the reason why the impurity binding energy increases with increase in the dielectric constant ratio  $\epsilon$  [16]. The same situation happens in figure 4 for AlAs/GaAs and ZnTe/CdSe corners. Also, when the impurity is far from the corner, the confinement of electron by the potential barrier is very weak, the image potentials due to dielectric mismatch become small, and the electronic wavefunctions for impurity states in the corner tend to the wavefunction in the bulk; this means that the impurity binding energy tends to the bulk value.

Summing up, we have investigated electronic and shallow impurity states in the corners, including the image potentials. The results show that localized electronic states exist when the dielectric mismatch  $p$  between the well materials and barrier material is negative, and the ground-state level increases with increase in the dielectric mismatch  $p$ . The results also show that the impurity binding energy tends to the value of the third impurity excited states in the bulk when the impurity is very near the corner. Because of the existence of localized electronic states when the dielectric mismatch  $p$  is negative and the variations in impurity binding energy with impurity position near the corner, the optical transition spectra will be changed around an interface when stepped structures exist in the interface. This will be investigated in a forthcoming paper.

### Acknowledgments

The authors would like to thank Dr Zhong-Ling Peng for a valuable discussion.

### References

- [1] Weisbuch C, Dingle R, Gossard A C and Weigmann W 1980 *J. Vac. Sci. Technol.* **17** 1128
- [2] Fujiwara K, Kanamoto K and Tsukada N 1989 *Phys. Rev. B* **40** 9698
- [3] Tanaka M and Sakaki H 1988 *Japan. J. Appl. Phys.* **27** L2025
- [4] Tanaka M and Sakaki H 1989 *Appl. Phys. Lett.* **54** 1326
- [5] Tsuchiya M, Gaines J M, Yan R H, Simes R J, Holtz P O, Coldren L A and Petroff P M 1989 *Phys. Rev. Lett.* **62** 466
- [6] Khoo G S and Ong C K 1993 *J. Phys.: Condens. Matter* **5** 6507
- [7] Namba H, Nakanishi N, Yamaguchi T and Kuroda H 1993 *Phys. Rev. Lett.* **71** 4027
- [8] Lee W W and Antoniewicz P R 1989 *Phys. Rev. B* **40** 3352
- [9] Lee W W and Antoniewicz P R 1989 *Phys. Rev. B* **40** 9920
- [10] Shen Z J, Yuan X Z, Yang B C and Shen Y 1993 *Phys. Rev. B* **48** 1977
- [11] Mailhot C, Chang Y C and McGill T C 1982 *Phys. Rev. B* **26** 4449
- [12] Madelung O 1982 *Landolt-Bernstein New Series, Zahlenwerte und Funktionen aus Naturwissenschaften und Technik Neue Serie Group III vol 17* (Berlin: Springer)
- [13] Elabasy A M 1992 *Phys. Rev. B* **46** 2621



- [14] Lee H J, Juravel L Y and Wooly J C 1980 *Phys. Rev. B* **21** 659
- [15] Luo H, Samarth H, Zhang F C, Pareek A, Dobrowolska M, Furdyna J K, Mahalingam K, Otsuka N, Chou W C, Petrou A and Qadri S B 1991 *Appl. Phys. Lett.* **58** 1783
- [16] Deng Z Y and Gu S W 1993 *Phys. Rev. B* **48** 8083